Eur. Phys. J. C 9, 511–520 (1999)
Digital Object Identifier (DOI) 10.1007/s100529900008

THE EUROPEAN PHYSICAL JOURNAL C

Associated stop-Higgs production at a linear collider and extraction of stop parameters

G. Bélanger[1], F. Boudjema[1], T. Kon[2], V. Lafage[3]

[1] Laboratoire de Physique Théorique LAPTH[a], Chemin de Bellevue, B.P. 110, F–74941 Annecy-le-Vieux, Cédex, France
[2] Seikei University, Musashino, Tokyo 180–8633, Japan
[3] High Energy Accelerator Research Organisation, KEK, Tsukuba, Ibaraki 305–801, Japan

Received: 19 November 1998 / Published online: 18 June 1999

Abstract. We calculate stop-stop-Higgs production at a linear collider. Combining the measurements from the pair production of the lightest stop and that of the mass of the Higgs, we show how, in a scenario where only the lightest stop and the lightest Higgs are accessible, one could extract the mass of the heavier stop and infer some useful information on the supersymmetric parameters.

1 Motivation and stop mass parameters

The elucidation of the mechanism of symmetry-breaking, alongside the discovery of the Higgs and the study of its properties, are the prime motivations for the construction of future colliders. It is well known that the standard description of the Higgs sector in the Standard Model ($\mathcal{SM}$) is unsatisfactory, while the implementation of supersymmetry (SUSY) provides an elegant solution to the naturalness problem. Moreover, SUSY can be made consistent with all present data [1], and offers as a bonus a successful framework for the gauge couplings unification. Contrary to the $\mathcal{SM}$, SUSY predicts an upper bound for the lightest Higgs, within reach of the upcoming LHC and linear colliders, and perhaps even LEP2 and the Tevatron. The top-stop sector plays a crucial role in that it can contribute large radiative corrections to the tree-level mass of this Higgs [2–6]. Studying the top-stop connection to the Higgs and electroweak symmetry- breaking, $\mathcal{SB}$, is also important for a number of reasons. In many SUSY scenarios, like the popular mSUGRA [7], a heavy top can very nicely trigger $\mathcal{SB}$. Recently there has been a renewed interest in the possibility of having a light stop, which in many scenarios can be the lightest scalar beside the Higgs. With strong couplings to the Higgs, a light stop can make electroweak baryogenesis work [8]. In another context, it has been pointed out that if the mixing in the stop sector is quite large, and a lightest stop is present that has a mass of the order of the top mass or less, it may be impossible to detect the lightest Higgs through the classic two- photon decay at the Large Hadron Collider (LHC) [9]. Therefore, there is clearly ample motivation for the direct study of the stop-Higgs coupling. The latter should be considered as important as the study of the tth vertex through $e^+e^- \to tth$ [10]. Because the light stops that we will be considering will decay into hadrons, we feel that for the precision measurements of the couplings, a linear collider[11–14], especially with a high luminosity as is currently planned [12], is best suited. Higgs radiation off light stops at the LHC has been studied in [15], but not from the perspective of extraction of the SUSY parameters.

Our aim in the present paper is not only to give the cross section for $\tilde{t}_1\tilde{t}_1 h$ production at a moderate energy e^+e^- but also to inquire what we may learn from such a measurement. For instance, one should ask which SUSY parameters one can hope to extract, especially when this process is combined with other measurements that will certainly be made at the same machine. This includes $\tilde{t}_1\tilde{t}_1$ production and a prior determination of the Higgs mass. To further strengthen our motivations we will be considering a scenario in which, besides the lightest Higgs, the lightest stop is the next-to-lightest SUSY particle. If this scenario occurs, then within an R-parity conserving model, besides the lightest neutralino acting as the lightest supersymmetric particle (LSP), one may only observe the lightest stop, $\tilde{t}_1$, and the Higgs in a first-stage e^+e^- linear collider. Although this may look meager from the perspective of discovery, one should inquire whether we can exploit the few cross sections and observables to extract some of the basic parameters of the model and infer some information on those particles which are not directly accessible. The purpose of this analysis is to show how this could be done by exploiting both indirect effects present in the radiative corrections to the Higgs mass and a subdominant cross section, $e^+e^- \to \tilde{t}_1\tilde{t}_1 h$, which a high luminosity e^+e^- with a clean environment allows.

[a] URA 14–36 du CNRS, associée à l'Université de Savoie

2 Stop parameters and $e^+e^- \to \tilde{t}_1\tilde{t}_1$

To discuss the stop sector and define our conventions, we turn to the weak eigenstate basis where the mass matrix in the $\tilde{t}_L$, $\tilde{t}_R$ involves the the SUSY soft-breaking masses; the common SU(2) mass $\tilde{m}_{\tilde{Q}_3}$, the U(1) mass $\tilde{m}_{\tilde{U}_{3R}}$, and the mixing, $\tilde{m}^2_{\tilde{t}_{LR}}$

$$\begin{aligned} m^2_{\tilde{t}_L} &= \tilde{m}^2_{\tilde{Q}_3} + m_t^2 \\ &\quad + \frac{1}{2}M_Z^2\left(1 - \frac{4}{3}\sin^2\theta_W\right)\cos(2\beta) \qquad (2.1) \\ m^2_{\tilde{t}_R} &= \tilde{m}^2_{\tilde{U}_{3R}} + m_t^2 + \frac{2}{3}M_Z^2\sin^2\theta_W\cos(2\beta) \\ m^2_{\tilde{t}_{LR}} &= -m_t\left(A_t + \frac{\mu}{\tan\beta}\right) \qquad (2.2) \end{aligned}$$

One sees that apart from the soft SUSY-breaking parameters $\tilde{m}_{\tilde{Q}_3}$, $\tilde{m}_{\tilde{U}_{3R}}$, and the tri-linear top term (A_t), there appears also the ubiquitous $\tan\beta$ and the Higgsino mass term μ. In principle, $\tan\beta$ and μ could be reconstructed from a study of chargino and heavy neutralino cross sections [16–18] but in the scenario that we are investigating with only a light Higgs and a light stop besides the LSP[1], these may not be accessible[2]. However, non- observation of an unstable chargino/neutralino would mean that $|\mu|$ and $|M_2|$ (the gaugino mass parameter) are large. We will take this constraint into account. The stop mass eigenstates are defined through the mixing angle $\theta_{\tilde{t}}$, with the lightest stop, $\tilde{t}_1$,

$$\tilde{t}_1 = \cos\theta_{\tilde{t}}\,\tilde{t}_L + \sin\theta_{\tilde{t}}\,\tilde{t}_R \qquad (2.3)$$

In our case, since we are aiming at reconstructing the physical masses, we find it useful to express the mixing angle as:

$$\sin(2\theta_{\tilde{t}}) = \frac{2\,m^2_{\tilde{t}_{LR}}}{m^2_{\tilde{t}_1} - m^2_{\tilde{t}_2}} \qquad (2.4)$$

The tree-level amplitude for $\tilde{t}_1$ pair production with a left-handed (right-handed) electron $\mathcal{M}_{L(R)}$ may be written as [19,20]:

$$\begin{aligned} \mathcal{M}_L &= \mathcal{M}_0\left(\frac{2}{3} + \frac{1}{s_W^2 c_W^2}\left(\frac{1}{2} - s_W^2\right)\times\right. \\ &\qquad \left.\left(\frac{1}{2}\cos^2\theta_{\tilde{t}} - \frac{2}{3}s_W^2\right)\frac{s}{s - M_Z^2}\right) \\ \mathcal{M}_R &= \mathcal{M}_0\left(\frac{2}{3} - \frac{1}{c_W^2}\left(\frac{1}{2}\cos^2\theta_{\tilde{t}} - \frac{2}{3}s_W^2\right)\frac{s}{s - M_Z^2}\right) \end{aligned} \qquad (2.5)$$

$\mathcal{M}_0$ is completely given in terms of gauge couplings. With $\sin^2\theta_W = 1/4$ and $s \gg M_Z^2$, this simplifies, for the $\tilde{t}_1$, to

$$\begin{aligned} \mathcal{M}_L &\simeq \frac{2}{3}\mathcal{M}_0\left(\frac{2}{3} + \cos^2\theta_{\tilde{t}}\right) \\ \mathcal{M}_R &\simeq \frac{2}{3}\mathcal{M}_0\left(\frac{4}{3} - \cos^2\theta_{\tilde{t}}\right). \end{aligned} \qquad (2.6)$$

We see from the $e^+e^- \to \tilde{t}_1\tilde{t}_1$ cross section that only the $\cos^2\theta_{\tilde{t}}$ can be measured. Previous studies and simulations (see for instance [11,21,22]) have shown that with a very moderate luminosity this angle can be measured at the few-percent level ($\simeq 3-4\%$); with the high luminosity envisaged by the new TESLA design (500 fb^{-1}), we can do much better[3]. Although this measurement of the cosine will come with a sign ambiguity, we will see that, in fact, for most cases of interest, one needs only the square of the cosine for the calculation of the $\tilde{t}_1\tilde{t}_1 h$ cross section. The unpolarized $\tilde{t}_1\tilde{t}_1$ cross section is (for a fixed stop mass) lowest for $\cos^2\theta_{\tilde{t}} \simeq 1/3$. For this value, the L and R cross sections are equal. For larger $\cos^2\theta_{\tilde{t}}$, production with a left-handed electron dominates. Incidentally, the same beam polarization which makes the $\tilde{t}_1\tilde{t}_1$ largest makes the $\tilde{t}_1\tilde{t}_1 h$ larger also, as we will discuss. From a threshold scan we can easily infer the (physical) mass of the stop, whereas one can measure $\cos^2\theta_{\tilde{t}}$ from the absolute value of the cross section or a ratio of the left-handed/right-handed cross Sect. [19]. In principle, depending on the mass of the stop and its decays, one can also extract useful information and constrain some parameters [22]. To set an order of magnitude for the cross section, we see that one should expect cross sections of the order of 100 fb at 500 GeV center-of-mass energy.

3 $e^+e^- \to \tilde{t}_1\tilde{t}_1 h$ production

$e^+e^- \to \tilde{t}_1\tilde{t}_1 h$ production proceeds via three kinds of diagrams (See Fig. 1). The most important is a bremsstrahlung of a Higgs off $\tilde{t}_1$, which involves the $\tilde{t}_1\tilde{t}_1 h$ vertex (Diag. 1–4 in Fig. 1). One also has the conversion of $\tilde{t}_2$ to $\tilde{t}_1$, which involves the $\tilde{t}_2\tilde{t}_1 h$ vertex. Though this contribution turns out to be small, there are some regions in the parameter space where it cannot be neglected. One last type is hZ^* production with $Z^* \to \tilde{t}_1\tilde{t}_1$. The latter can be predicted precisely once $e^+e^- \to Zh$ and $e^+e^- \to \tilde{t}_1\tilde{t}_1$ have been measured, but this contribution is totally negligible. The fact that the cross section is dominated by the bremsstrahlung off the lightest stop explains why the effect of beam polarization on this process is almost the same as that on the light-stop pair production. Since diagrams involving $\tilde{t}_1\tilde{t}_1 h$ are dominant and could allow us to

[1] This will then be mostly a bino.

[2] Of course, by the time the linear collider (LC) is running one may have some useful information on the SUSY parameters from the LHC, for instance.

[3] We also note that for a given $\cos^2\theta_{\tilde{t}}$, the precision on its measurement improves as $1/\sqrt{\mathcal{L}}$, assuming that the experimental error is set by the statistics. Ultimately one needs a simulation similar to [21] that takes into account the impact of the QCD radiative corrections [23,24] together with ISR and exploits the benefits of polarization in the environment of a high luminosity option of the LC.

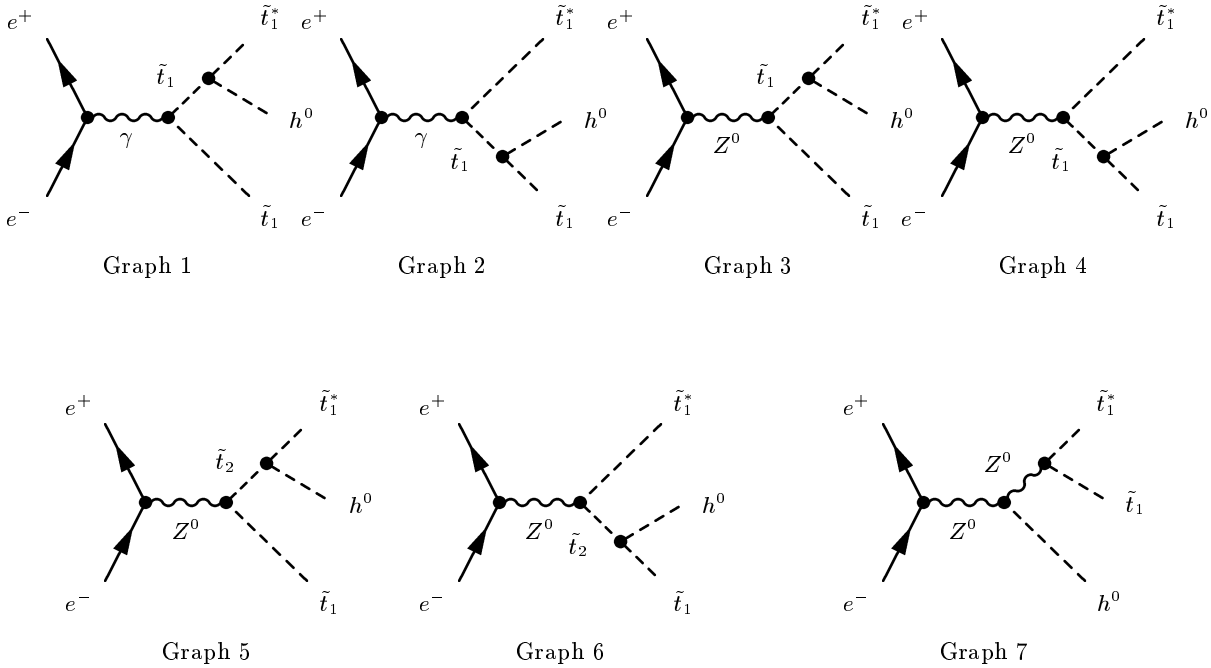

Fig. 1. Feynman graphs contributing to $e^+e^- \to \tilde{t}_1\tilde{t}_1 h$

reconstruct the mass of the $\tilde{t}_2$, let us study this vertex in detail.

3.1 The $\tilde{t}_1\tilde{t}_1 h$ vertex

The stop-stop Higgs couplings, like the stop mass matrix, emerge essentially from the F-terms in the scalar potential (there is a residual D term component $\propto M_Z^2$). With the angle α in the Higgs mixing matrix, the $\tilde{t}_1\tilde{t}_1 h$ coupling is (we write the potential):

$$V_{\tilde{t}_1\tilde{t}_1 h} = -g\frac{m_t}{M_W}\frac{\cos\alpha}{\sin\beta}\Big[(A_t^\star - \mu\tan\alpha)\sin\theta_{\tilde{t}}\ \cos\theta_{\tilde{t}} \ -\ m_t + \frac{M_Z^2}{m_t}\frac{\sin\beta}{\cos\alpha}\sin(\alpha+\beta)\left(\left(\frac{1}{2}-\frac{2}{3}\sin^2\theta_W\right)\cos^2\theta_{\tilde{t}} + \frac{2}{3}\sin^2\theta_W\sin^2\theta_{\tilde{t}}\right)\Big]. \quad (3.1)$$

The vertex does involve some important parameters which stem from the Higgs sector, notably the angle α. Since we will be working in a scenario where at 500 GeV, only the lightest Higgs has been observed, we are in the the decoupling limit of large M_A. Actually it has been shown that this decoupling limit is reached for very moderate masses of M_A [25]. In this limit and up to radiative corrections we have

$$\tan\alpha\ \tan\beta = -1, \quad (3.2)$$

from which we write,

$$\tan\alpha\tan\beta = -(1+r) \qquad \text{with} \qquad r \ll 1 \quad (3.3)$$

where r collects all M_A dependence and other radiative corrections which also occur in the computation of the Higgs masses. We will return to the issue of how small r is and what parameters influence r, but for the moment, let us observe that for small r, the coupling as written in (3.1) may be cast into

$$V_{\tilde{t}_1\tilde{t}_1 h} = +gR\frac{1}{M_W}\Big\{m_t^2 + \sin\theta_{\tilde{t}}\ \cos\theta_{\tilde{t}}\left(\sin\theta_{\tilde{t}}\ \cos\theta_{\tilde{t}}(m_{\tilde{t}_1}^2 - m_{\tilde{t}_2}^2) - \frac{m_t\ \mu\ r}{\tan\beta}\right) + M_Z^2\big((2+r)\cos^2\beta - 1\big)\left(\left(\frac{1}{2}-\frac{2}{3}\sin^2\theta_W\right)\cos^2\theta_{\tilde{t}} + \frac{2}{3}\sin^2\theta_W\sin^2\theta_{\tilde{t}}\right)\Big\}$$

$$\text{with } R = \frac{\cos\alpha}{\sin\beta} \quad \text{and} \quad R^2 = \frac{1+\tan^2\beta}{1+\tan^2\beta+r^2+2r} \qquad R \simeq 1 - \frac{r}{1+\tan^2\beta}. \quad (3.4)$$

We see that in the limit $r \ll 1$, where r is neglected, the $\tilde{t}_1\tilde{t}_1 h$ simplifies greatly when written in terms of the measurable parameters $m_{\tilde{t}_1}$, $m_{\tilde{t}_2}$ and $\cos^2\theta_{\tilde{t}}$. It is important to realize that, neglecting the correction due to r, the coupling no longer depends on μ. Notice also in (3.4) that this correction is reduced as $\tan\beta$ gets larger. However, as $\tan\beta$ gets larger ($\tan\beta > 25$), effects of the sbottoms in correcting both the vertex and the prediction of the Higgs mass start becoming significant (r may not be neglected in this case). Discarding the r correction altogether, we end up with a compact formula where the only two unknowns (once $e^+e^- \to \tilde{t}_1\tilde{t}_1$ has been measured) are $\tan\beta$ and $m_{\tilde{t}_2}$,

the mass of the heavier stop. In this approximation we get

$$V_{\tilde{t}_1\tilde{t}_1 h} \simeq \frac{g}{M_W}\Big\{\sin^2\theta_{\tilde{t}}\,\cos^2\theta_{\tilde{t}}\,(m^2_{\tilde{t}_1}-m^2_{\tilde{t}_2})\;+\;m_t^2 + M_Z^2\cos(2\beta)\Big(\Big(\frac{1}{2}-\frac{2}{3}\sin^2\theta_W\Big)\cos^2\theta_{\tilde{t}} +\frac{2}{3}\sin^2\theta_W\sin^2\theta_{\tilde{t}}\Big)\Big\} \quad (3.5)$$

It should be further noted that the explicit $\tan\beta$ dependence in the vertex can be considered subdominant as compared to the m_t^2 term. This remaining small D-term contribution is mildly dependent on $\tan\beta$, so long as $\tan\beta > 2$, and for values of the stop masses and mixing such that there is a measurable $\tilde{t}_1\tilde{t}_1 h$ cross section (see below). Of course, the Higgs mass does depend quite strongly on $\tan\beta$, and this is where the main $\tan\beta$ dependence at the level of the $\tilde{t}_1\tilde{t}_1 h$ cross section may be felt. We have verified explicitly that the use of (3.5) is excellent as compared to the exact (fully corrected) vertex. The approximation is always within 2% for all values of the stop masses and mixings that give an observable $\tilde{t}_1\tilde{t}_1 h$ cross section at a high-luminosity linear collider, as long as $\tan\beta < 25$ for a wide scan on the sbottom masses and μ. The value of r is also below 2% for $\tan\beta < 25$ (the sbottom contribution is then small); we find that the maximum of r, $r = 1.9\%$, occurs for $\tan\beta = 2, m_A = 1$ TeV, $\mu = 1.1$ TeV, and $m_{\tilde{t}_2} = 900$ GeV. Thus the vertex hardly shows a sensitivity to μ. We also confirm that the $\tan\beta$ dependence in the vertex is also hardly noticeable, thus, considering the statistical error with which the cross section of interest will be measured, the vertex will depend essentially on the heavier stop mass (after inputting the mixing angle and the lightest stop mass.)

Equation (3.5) makes it clear that the vertex (and hence the cross section) will be largest for maximal mixing, $\sin^2 2\theta_{\tilde{t}} \sim 1$ ($\cos\theta_{\tilde{t}} \sim 0.7$). A sharp dip in the vertex occurs (that will also be reflected in the cross section) when the stop contribution and that of the top cancel each other. This occurs for values of the mixing angle such that

$$\sin^2 2\theta_{\tilde{t}} \simeq \frac{4m_t^2}{m^2_{\tilde{t}_2}-m^2_{\tilde{t}_1}}. \quad (3.6)$$

On the other hand, when the mixing is negligible, the vertex is accounted for almost entirely by the top mass and therefore has the same strength as the tth vertex. In this situation we expect that if the mass of the lightest stop and that of the top are of the same order, then so would the cross sections for tth and $\tilde{t}_1\tilde{t}_1 h$ production. Indeed, the tth vertex has strength

$$V_{tth} = \frac{g}{2M_W} R\, m_t. \quad (3.7)$$

Associated production of Higgses with tops has been studied previously [10]. Returning for a moment to the issue large $\tan\beta$, and the sbottom *contamination* in the correction to the vertex and the Higgs mass, it is worth pointing out that this entails a not-so-negligible r. However, the latter may be measured in the couplings of the Higgs to fermions and bosons. In fact, the best way to measure r in this case would be through a precision measurement of the Higgs decay into $b\bar{b}$; this involves the coupling $R' = R(1+r)$ which is more sensitive to r than R is, and $h \to b\bar{b}$ would have by far the best statistics. In the same vein, note that Zh production may not serve as a good measure of r, despite its statistics, since the ZZh vertex has a (small) quadratic dependence in r:

$$\sin^2(\alpha-\beta) \simeq 1\;-\;r^2\frac{\tan\beta^2}{(1+\tan\beta^2)^2}. \quad (3.8)$$

Therefore, if r is not so small, it could be extracted from measurements of the Higgs couplings to, e.g., $b\bar{b}$[4], this can then be combined with the measurements of the cross sections that we are considering and the Higgs mass to constrain the SUSY parameters.

One further point should be noted. As we pointed out above, measurement of stop pair does not measure the absolute value of $\cos\theta_{\tilde{t}}$, only $\cos^2\theta_{\tilde{t}}$. It is gratifying to see that if one neglects the small correction $m_t\,\mu\,r/\tan\beta$, the $\tilde{t}_1\tilde{t}_1 h$ vertex depends on the quantity $\sin^2\theta_{\tilde{t}_1}\cos^2\theta_{\tilde{t}_1}$, that is, the squares of the mixing in the stop parameters which is exactly what is measured from $\tilde{t}_1\tilde{t}_1$ production. This, together with the fact that the $\tilde{t}_1\tilde{t}_1 h$ vertex combines, at the amplitude level, with $\tilde{t}_1\tilde{t}_1 Z$, which is proportional to $\cos^2\theta_{\tilde{t}} - 4/3\sin^2\theta_W$ (and the $\tilde{t}_1\tilde{t}_1\gamma$ which is independent of the mixing angle), means that the sign of $\cos\theta_{\tilde{t}}$, which is not measured in stop-pair production, is not critical in computing the the $\tilde{t}_1$ exchange diagrams in the decoupling limit.

3.2 Influence of the $\tilde{t}_2$ exchange diagrams

A similar conclusion to that drawn in Sect. 3.1 holds for the amplitudes involving $\tilde{t}_2$ exchange. Indeed, the $\tilde{t}_1\tilde{t}_2 h$ vertex may be cast into

$$V_{\tilde{t}_1\tilde{t}_2 h} = +gR\frac{1}{M_W}\Big\{\frac{\cos 2\theta_{\tilde{t}}}{4}\Big(\sin 2\theta_{\tilde{t}}\,(m^2_{\tilde{t}_1}-m^2_{\tilde{t}_2}) - \frac{2m_t\,\mu\,r}{\tan\beta}\Big) + M_Z^2\sin 2\theta_{\tilde{t}}\,(\cos 2\beta + r\cos^2\beta)\Big(\frac{2}{3}\sin^2\theta_W - \frac{1}{4}\Big)\Big\}. \quad (3.9)$$

Within the approximation that neglects the r terms, the full $\tilde{t}_2$ exchange diagram, when combined with the $\tilde{t}_1\tilde{t}_2 Z$ vertex, only requires the knowledge of $\cos^2\theta_{\tilde{t}}$. Note that the term in m_t^2 does not appear in the off-diagonal vertex. In the large $m_{\tilde{t}_2}$ limit where the vertex grows large, the $m_{\tilde{t}_2}$ dependence is off-set by that of the propagator. The $\tilde{t}_2$ contribution, though much smaller than that of the dominant $\tilde{t}_1$ exchange diagrams, may not always be

[4] A similar conclusion was reached in [26] who considered an expansion of the Higgs couplings in $1/M_A$ and $1/\tan\beta$.

neglected. For instance, take the case of a center-of-mass energy of 500 GeV, with $\mu = 400$ GeV. With $\tan\beta = 10$, $\cos\theta_{\tilde{t}} = 0.4$, and $m_{\tilde{t}_1} = 800$ GeV, we find a total cross section of 0.78 fb, of which 90% is accounted for by the $\tilde{t}_1$ diagrams alone (graphs 1–4 in Fig. 1). The $\tilde{t}_2$ diagrams by themselves are more than two orders of magnitude smaller than the diagrams with virtual $\tilde{t}_1$ exchange while the diagram with the vertex ZZh is a further two orders of magnitude smaller. We find that there are points in the parameter space where, through interference, the $\tilde{t}_2$ diagrams should be taken into account, while the Zh-type is invariably always negligible. This said, one should take into account that the cross sections are rather small, and even for a high luminosity of 500 fb^{-1}, neglecting the $\tilde{t}_2$ contribution hardly amounts to more than a 2σ deviation, assuming an efficiency of 50%.

3.3 The Higgs mass dependence and measurement of $\tan\beta$

We have argued that for values of the stop masses and mixings which entail a large enough stop-Higgs coupling and hence a large cross section, the $\tan\beta$ dependence in the vertex is negligible. However, the Higgs mass crucially depends on this parameter, besides the corrections to the tree-level formula which involve the stop parameters. In our calculation we have taken $\tan\beta$, $m_{\tilde{t}_1}$, $m_{\tilde{t}_2}$, $\cos\theta_{\tilde{t}}$ and μ as input parameters. This allows us to calculate both the vertices and the Higgs mass in the decoupling limit, with the assumption of vanishing sbottom contributions, which we found to hold very well, so long as $\tan\beta$ is smaller than ~ 25. In this case, the same parameters that specify the $\tilde{t}_1\tilde{t}_1h$ vertex fix the Higgs mass[5]. Although in our analysis we have used numerical formulae for the corrected Higgs mass (based on [3], but with a running top mass to effectively incorporate the leading two-loop corrections [4][6]), it is instructive to appeal to the following one-loop approximation to exhibit the dependence of the Higgs mass on the stop parameters and help in the discussion (where also the mass of the top is understood as running [5]):

$$
\begin{aligned}
m_h^2 &= M_Z^2\cos^2(2\beta) \\
&\quad + \frac{3\alpha}{4\pi\sin^2\theta_W}\frac{\bar{m}_t^4}{M_W^2}\left(\log\left(\frac{m_{\tilde{t}_1}^2\, m_{\tilde{t}_2}^2}{m_t^4}\right) + \right. \\
&\qquad \left(\sin^2\theta_{\tilde{t}}\cos^2\theta_{\tilde{t}}\frac{(m_{\tilde{t}_1}^2 - m_{\tilde{t}_2}^2)}{m_t^2}\right)^2 \times f(m_{\tilde{t}_2}^2, m_{\tilde{t}_1}^2) \\
&\qquad \left. +2\sin^2\theta_{\tilde{t}}\cos^2\theta_{\tilde{t}}\frac{(m_{\tilde{t}_1}^2 - m_{\tilde{t}_2}^2)}{m_t^2}\log(m_{\tilde{t}_1}^2/m_{\tilde{t}_2}^2)\right) \\
f(x,y) &= 2 - (x+y)/(x-y)\log(x/y). \qquad (3.10)
\end{aligned}
$$

[5] This is to be expected: cutting the one-loop diagram contributions to the Higgs mass from the top-stop sector gives the vertices that enter the calculation of $e^+e^- \to \tilde{t}_1\tilde{t}_1h$.

[6] A more complete analysis needs to incorporate the results of more complete two-loop corrections [6].

The latter analytical approximation shows that the combinations of parameters that enter into the $\tilde{t}_1\tilde{t}_1h$ vertex and the Higgs mass are the same, and more importantly, that there is no μ dependence. In fact, the numerical estimates show a very mild μ dependence (in the limit of no sbottom contributions). Varying $|\mu|$ from 400 GeV to 1 TeV changes the Higgs mass by a few per-mil. The lower value of 400 GeV was set so that Higgsinos would be too heavy to be produced at a 500 GeV e^+e^-.

3.4 Constraints from low Higgs masses, $\Delta\rho$, CCB and the influence of sbottoms

Large values of the $\tilde{t}_1\tilde{t}_1h$ vertex, which lead to the largest cross sections occur for maximal mixing with a large splitting between the physical masses of the stops. However, it is for this configuration that some strong constraints preclude the highest values of the cross section. For instance, one needs to be aware that imposing a lower bound on the Higgs mass, from its non-observation at, say, LEP2, can restrict drastically the $\cos\theta_{\tilde{t}} - m_{\tilde{t}_2}$ parameter space. This constraint is very much dependent on $\tan\beta$. Much less dependent on $\tan\beta$, but a quite powerful for the values of $m_{\tilde{t}_1}$ that we have entertained, is the constraint coming from $\Delta\rho$ [27]. Taking the present limit $\Delta\rho < 0.0013$ (applicable to New Physics) with a light Higgs [1], which here means essentially the contribution from stops and sbottoms (and marginally the Higgs sector in our decoupling scenario[7]), generally excludes region of the parameter space where the $\tilde{t}_1\tilde{t}_1h$ is largest. In implementing the constraint from $\Delta\rho$, we have taken $m_{\tilde{b}_1} = 300$ GeV and scanned over μ, as above. In our study, the mixing in the sbottom has always been assumed to be zero.

To illustrate the effect of these constraints, let us concentrate on the case study at 500 GeV, with $m_{\tilde{t}_1} = 120$ GeV and $m_{\tilde{b}_1} = 300$ GeV. For $m_{\tilde{t}_2} = 700$ GeV, the lower bound $m_h > 90$ GeV means that maximal mixing for large $\tan\beta$, say $\tan\beta = 10$, is excluded; we find that the range $0.67 < \cos\theta_{\tilde{t}} < 0.73$ is not compatible with this lower bound on the Higgs mass, whereas for $\tan\beta = 2$ the allowed range is $0.17 < \cos\theta_{\tilde{t}} < 0.53$ and $0.85 < \cos\theta_{\tilde{t}} < 0.99$. The range $0.54 < \cos\theta_{\tilde{t}} < 0.94$ and $0.98 < \cos\theta_{\tilde{t}} < 1$ is excluded by $\Delta\rho$ (almost independent of $\tan\beta$). Putting the two constraints, $m_h > 90$ GeV and $\Delta\rho < 0.0013$, together means that the allowed range is

$$
\begin{aligned}
&\bullet\ \tan\beta = 10: && 0.0 \quad < \cos\theta_{\tilde{t}} < 0.54 \\
&\qquad\qquad\ \text{and} && 0.94 < \cos\theta_{\tilde{t}} < 0.98 \\
&\bullet\ \tan\beta = 2: && 0.17 < \cos\theta_{\tilde{t}} < 0.53 \\
&\qquad\qquad\ \text{and} && 0.94 < \cos\theta_{\tilde{t}} < 0.98 \qquad (3.11)
\end{aligned}
$$

For large $\tan\beta$, the constraint comes essentially from $\Delta\rho$, whereas for $\tan\beta = 2$, the constraint is from the Higgs

[7] For light stops in the decoupling limit, the sbottom-stop contribution, when substantial, gives a positive contribution, whereas the Higgs sector contributes a negligible negative contribution. The minuscule μ dependence in $\Delta\rho$ enters indirectly in the latter contribution.

mass. As the mass of the heavier stop increases, these ranges narrow. For instance, the above limit of 0.54 for $\tan\beta = 10$ moves to .48 for $m_{\tilde{t}_2} = 800$ GeV. On the other hand, for moderate values of the mixing angle, all of the above constraints constitute mild restrictions. For instance, for $\cos\theta_{\tilde{t}} = 0.4$, the only strict condition stems from the Higgs mass. For $\tan\beta = 10$, this means that we should restrict ourselves to $m_{\tilde{t}_2} < 900$ GeV. For $\tan\beta = 2$, one has more "room" in the range $450 < m_{\tilde{t}_2} < 830$ GeV. Similar constraints hold for the analysis at $\sqrt{s} = 800$ GeV. Sticking to $m_{\tilde{t}_1} = 250$ GeV and $m_{\tilde{b}_1} = 400$ GeV, we find that for $\cos\theta_{\tilde{t}} = 0.4$ the constraints are mild and are set by the Higgs mass. For $\tan\beta = 10(2)$, we have $m_{\tilde{t}_2} < 1060(1000)$ GeV, this still allows us to probe $700 < m_{\tilde{t}_2} < 1000$ GeV. We will see that taking these constraints into account still allows for healthy cross sections, especially with a high-luminosity linear collider.

To be consistent, if we stick to our scenario that no sbottom has been observed, we should take into account that we have a lower bound on the sbottom mass, say half the center of mass energy. However, when the SU(2) squarks masses are equal, it is not always possible to have a light stop mass while keeping the lightest sbottom much heavier than the lightest stop. Indeed, since we are requiring the mixing angle in the sbottom sector to be small so that any residual sbottom dependence in the Higgs and $\tilde{t}_1\tilde{t}_1 h$ is small, one of the two sbottom masses sets the mass of the common SU(2) squark mass, up to D-terms. Therefore, when $\tilde{t}_1$ is mostly $\tilde{t}_L$ ($\cos\theta_{\tilde{t}} \simeq 1$), its mass approaches the common SU(2) mass when one allows for the top-mass contribution. Thus for $\cos\theta_{\tilde{t}} \simeq 1$, it is generally difficult to reconcile a very light stop with a much heavier sbottom, which would not have been pair- produced. At 500 GeV, the constraint from the sbottom mass requires $\cos\theta_{\tilde{t}} < 0.88$ and thus reduces the possible parameter space in (3.11) very little: The range $0.94 < \cos\theta_{\tilde{t}} < 0.98$ will not be allowed. Nonetheless, in this situation, where the left-handed sbottom may be produced, its mass, together with the measurements made in $e^+e^- \to \tilde{t}_1\tilde{t}_1$, may be used to extract $m_{\tilde{t}_2}$.

One more constraint needs mention. In the stop sector and in the presence of large mixing, as is the case here, one often has to check whether the parameters do not induce colour and charge- breaking global minima (CCB). To this end, the following condition has been proposed [28]:

$$A_t^2 < 3\left(\tilde{m}_{\tilde{Q}_3}^2 + \tilde{m}_{\tilde{U}_{3R}}^2 + (M_A^2 + M_Z^2)\cos^2\beta - \frac{1}{2}M_Z^2\right). \tag{3.12}$$

This constraint can sometimes slightly reduce the parameter space allowed by $\Delta\rho$ and the Higgs mass limit, as in (3.11). However, it has been argued that this condition may be too restrictive [29]. It has been shown that for a wide range of parameters, the global CCB minimum becomes irrelevant on the grounds that the time required to reach the lowest energy state exceeds the present age of the universe. Taking the tunneling rate into account, the above constraint (3.12) is relaxed, and can be replaced by the mild approximate constraint [29]:

$$A_t^2 + 3\mu^2 < 7.5(\tilde{m}_{\tilde{Q}_3}^2 + \tilde{m}_{\tilde{U}_{3R}}^2). \tag{3.13}$$

When presenting our results, we will, unless otherwise stated, impose the limits $m_h > 90$ GeV, $\Delta\rho < 0.0013$ together with the mild CCB constraint and the non-observation of sbottoms at the appropriate center-of-mass energies.

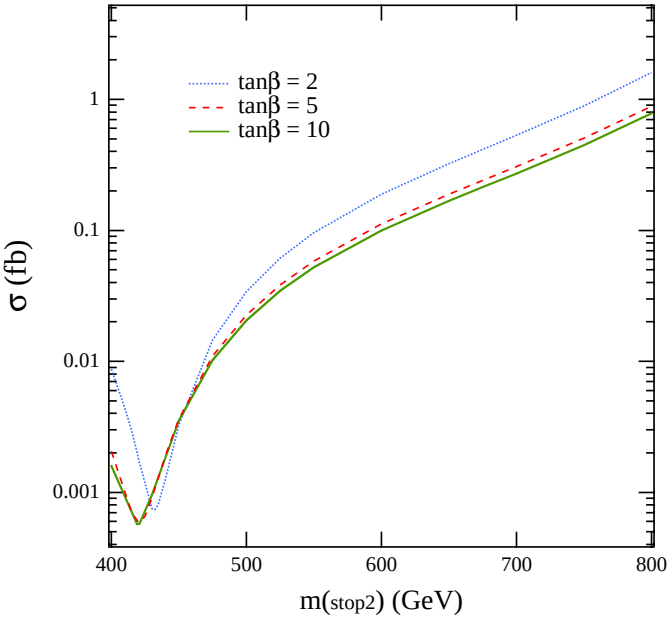

Fig. 2. $\tilde{t}_1\tilde{t}_1 h$ cross section at $\sqrt{s} = 500$ GeV as a function of $m_{\tilde{t}_2}$ for a fixed value of the mixing angle: $\cos\theta_{\tilde{t}}$=0.4 and $m_{\tilde{t}_1} = 120$ GeV. Right-handed electron polarization is chosen

4 Results and conclusions

The calculations have been done by using the package GRACE SUSY [30] for the automatic calculation of SUSY processes. We have adapted the package to include the radiative corrections to the Higgs mass and its couplings.

We start by describing a general feature of the cross section which is almost independent of the center-of-mass energy and the input parameters: the choice of the initial polarization. This choice very much depends on the value of the mixing angle and is controlled almost exclusively by the $\tilde{t}_1\tilde{t}_1$ cross section. This is easy to understand since $\tilde{t}_1\tilde{t}_1 h$ is dominated by the Higgs bremsstrahlung of $\tilde{t}_1$. Therefore, once the stop mixing angle has been measured, one should, for the purpose of enhancing $\tilde{t}_1\tilde{t}_1 h$, choose the most appropriate polarization that is also beneficial for $\tilde{t}_1\tilde{t}_1$ production. For example, for $\cos^2\theta_{\tilde{t}} < 1/3$, right-handed polarization is best. Let us now turn to how large a cross section we should expect at a 500 GeV collider. Because of the reduced-phase space, we have studied the

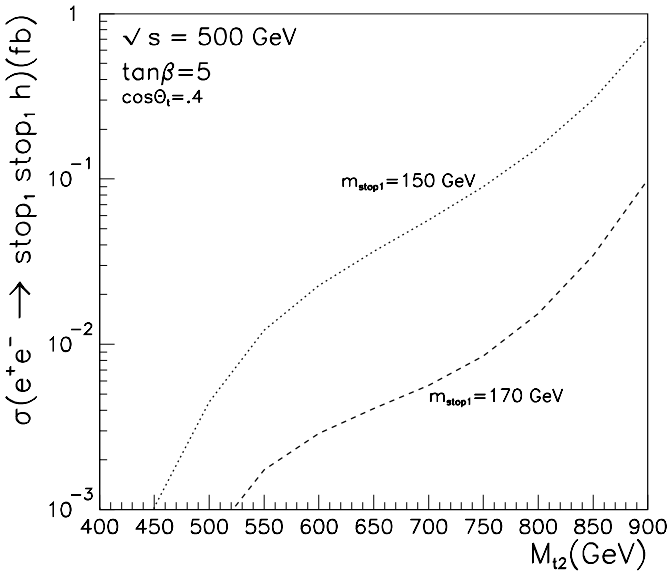

Fig. 3. Same as in the previous figure with $\tan\beta = 5$ and $m_{\tilde{t}_1} = 150, 170$ GeV

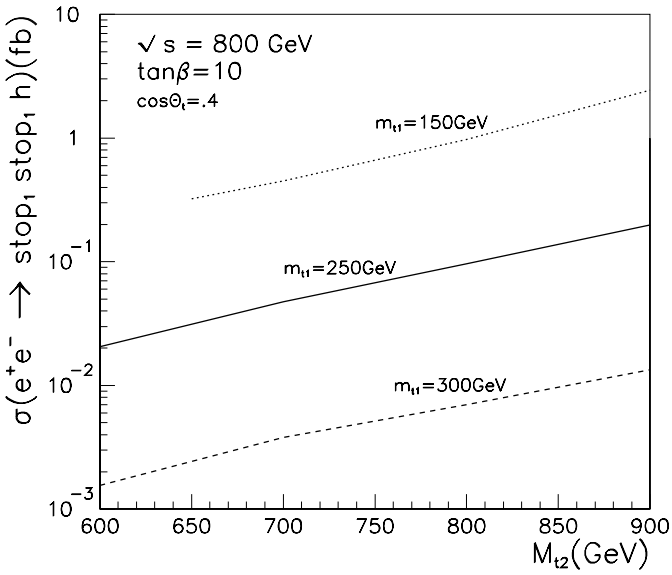

Fig. 4. Same as in the previous figure but at $\sqrt{s} = 800$ GeV for $\tan\beta = 10$ and three representative values of $m_{\tilde{t}_1}$. Note that for $m_{\tilde{t}_1} = 150$ GeV we only consider $\tilde{t}_2$ masses above threshold for $\tilde{t}_1\tilde{t}_2$ production

case with $m_{\tilde{t}_1} = 120$ GeV[8]. We will comment briefly on how our results change for higher masses. Fig. 2 shows that the expected yield depends strongly on the mass of the heavier stop for a moderate value of the stop mixing angle, $\cos\theta_{\tilde{t}} = 0.4$, compatible with all the constraints set in the previous section. The figure shows that for all values of $\tan\beta$, there is a sharp dip in the cross section. The latter dip corresponds to values of $\theta_{\tilde{t}}$, as given by (3.6), where the $\tilde{t}_1\tilde{t}_1 h$ vanishes. However, the cross section picks up quickly, and for $\tilde{t}_2$ masses larger than 550–600 GeV the cross section is larger than 0.1 fb, which is at the limit of observability with a luminosity of 50 fb^{-1}; thus it should be clearly observable with the high-luminosity TESLA option of 500 fb^{-1}. In fact, for yet larger stop masses, $m_{\tilde{t}_2} = 800$ GeV, the cross section is about 1 fb. These values depend very little on $\tan\beta$, whose effect is in fact reflected in the phase space because of its influence on the Higgs mass, and therefore lower values of $\tan\beta$ (with all other parameters fixed) give slightly larger cross sections because they are associated with lower Higgs masses. Note that, although the effect occurs for a value of the cross section too small to be observed, the location of the dip does show a slight $\tan\beta$ dependence. This is not surprising, since this effect occurs when the stops and top contributions in the vertex cancel each other out, hence the small D-term contribution may give a small contribution. At 500 GeV, the issue of phase space is crucial. As the mass of the lightest stop is increased, the cross section drops rather dramatically. For example, we show in Fig. 3 the cross section with $m_{\tilde{t}_1} = 150$ GeV and $m_{\tilde{t}_1} = 170$ GeV for $\tan\beta = 5$. We can see that, compared with the case where $m_{\tilde{t}_1} = 120$ GeV, the cross section drops by almost an order of magnitude for the favorable value of $m_{\tilde{t}_2} = 800$ GeV. If the mass of the lightest stop is increased further, even slightly, there is no hope of observing this process especially with a luminosity of 50 fb^{-1}. For higher $m_{\tilde{t}_1}$ one must go to higher energies. We illustrate this for the case of an 800 GeV center-of-mass energy in Fig. 4. At this energy one can hope to observe the process for $m_{\tilde{t}_1} = 250$ GeV if the mass of the heavier stop is large enough. Alternatively, we can look at this from the perspective of the extraction of the SUSY parameters: As the lightest stop gets heavier than the top, more and more decay channels open up, most importantly $\tilde{t}_1 \to t\tilde{\chi}_1^0$, which can also provide some information on the SUSY parameters. Note also that in our study, we have not considered values of the $\tilde{t}_2$ mass such that it can be produced in association with $\tilde{t}_1$, because in this case, one can have a direct measurement of the heavier stop mass. In this case, $\tilde{t}_2\tilde{t}_1$ can also trigger Higgs production through the decay of the heavier stop to the lighter one, and a Higgs, $\tilde{t}_2 \to \tilde{t}_1 h$, given appropriate values of the supersymmetric parameters, is produced.

Figure 5 makes clear which values of the heaviest stop can be extracted from a measurement of $\tilde{t}_1\tilde{t}_1 h$. Note that for a no-mixing scenario, the cross section, although relatively large, does not allow an extraction of the heavier stop mass. In this situation, the vertex is dominated by the top mass only; this explains why the cross section is of the same order of magnitude as the tth cross section. For large values of $\cos\theta_{\tilde{t}}$ (0.95), there is still a sensitive $m_{\tilde{t}_2}$ dependence. In this particular case, however, large values of $m_{\tilde{t}_2}$ ($m_{\tilde{t}_2} > 900$ GeV, see Fig. 5) are not allowed, due to the $\Delta\rho$ constraint. Moreover, in this scenario, SU(2)

[8] The present Tevatron limit is 122 GeV [31] but depends strongly on the assumed mass of the LSP neutralino and also on the mixing angle. Taking the LSP to be heavier than 37 GeV, this limit disappears.

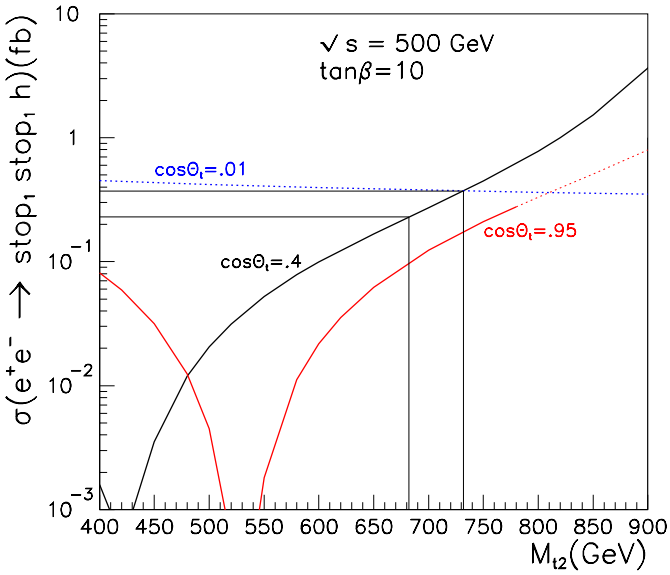

Fig. 5. Extraction of the heavier stop mass from $\tilde{t}_1\tilde{t}_1 h$. The figure gives the cross section at a centre-of-mass energy of 500 GeV as a function of the heavier stop mass and for different mixing angles. The 3σ measurement of the mass for a mixing angle $\cos\theta_t$=0.4 is also shown assuming a luminosity of 500 fb^{-1} and 50% detection efficiency. We have chosen the polarization of the e^+e^- such that one gets the largest cross section. For $\cos\theta_{\tilde{t}}$=0.4,0.01 we took right-handed electrons whereas for 0.95 we took left-handed electrons. Note that for the latter, the curve does not extend beyond $m_{\tilde{t}_2} \simeq 780$ GeV because of the constraint from $\Delta\rho$

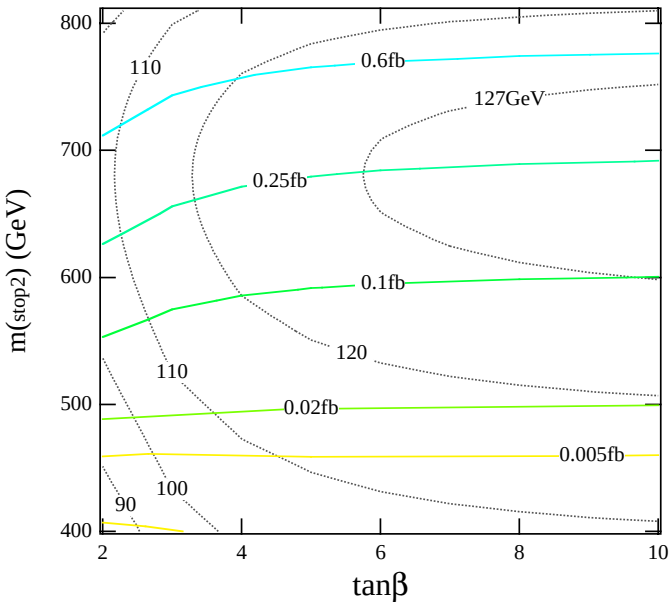

Fig. 6. Extraction of the heavier stop mass and $\tan\beta$ by combining the measurement of the cross section $\tilde{t}_1\tilde{t}_1 h$ (with right-handed electrons) with that of m_h at 500 GeV for $\cos\theta_{\tilde{t}} = 0.4$ and $m_{\tilde{t}_1} = 120$ GeV

symmetry on the squark masses requires an sbottom light enough to be produced at 500 GeV; as explained above, this allows an alternative measurement of $m_{\tilde{t}_2}$. Note once again the dramatic dip corresponding to (3.6). With a luminosity of 500 fb^{-1} and 50% detection efficiency, a 3σ measurement of the $\tilde{t}_1\tilde{t}_1 h$ cross section, for a cross section of 0.3 fb, restricts the mass of the heaviest stop to $694 < m_{\tilde{t}_2} < 737$ GeV for a mixing angle $\cos\theta_{\tilde{t}} = 0.4$. With the requirement of 10 raw events, a high luminosity e^+e^- will allow $m_{\tilde{t}_2} > 550(650)$ GeV to be probed for $\cos\theta_{\tilde{t}} = 0.4(0.95)$. We also see that for $\cos\theta_{\tilde{t}} = 0.95$, $m_{\tilde{t}_2} < 500$ GeV can be probed. Of course, unless there is very little mixing for $m_{\tilde{t}_2} < 400$ GeV, the heavier stop will be discovered through $\tilde{t}_1\tilde{t}_2$ production.

By combining the Higgs mass measurement and that of the $\tilde{t}_1\tilde{t}_1 h$, after having measured the stop mixing angle and the mass of the lighter stop in $e^+e^- \to \tilde{t}_1\tilde{t}_1$, it could be possible to extract both $m_{\tilde{t}_2}$ and $\tan\beta$. This is shown in Fig. 6 for $\cos\theta_{\tilde{t}} = 0.4$. A rough estimate based on a 3σ measurement of the $\tilde{t}_1\tilde{t}_1 h$ cross section indicates that an indirect measurement of both $m_{\tilde{t}_2}$ and $\tan\beta$ could be achieved at the 5% level. To provide a more realistic indication of how well the extraction of these parameters can be achieved, a thorough investigation is needed. Experimentally, one needs to determine how precisely the mass of the lightest stop and the mixing can be extracted from $\tilde{t}_1\tilde{t}_1$ production in a scenario where $\tilde{t}_1 \to c\tilde{\chi}_1^0$ almost exclusively. The issue of signatures and background is crucial. An analysis has been carried out in [21]. For the parameters that we have considered, we have verified that $\tilde{t}_1$ decays almost exclusively into $c\tilde{\chi}_1^0$ [32][9]. It is also essential to include the effects of radiative corrections, and to check that the latter can still allow the extraction of the mixing angle. Indeed, these corrections can introduce a few parameters that should be disentangled from the $\cos\theta_{\tilde{t}}$ dependence. For instance, it has been shown that though the gluonic corrections do not distort the $\cos\theta_{\tilde{t}}$ dependence, there is a slight distortion which depends on the gluino mass [24]. The latter contribution does, however, decrease with increasing gluino mass. Therefore, in our scenario either the gluino is light, and hence its mass measured, in which case this could be included in the simulation, or it is heavy, in which case it gives a slight contamination to the mixing angle determination. As for the use of m_h, we stress that we have used an improved one-loop approximation that involves only the stop parameters. A thorough investigation should include at least the full two-loop corrections [6]. Unfortunately, for some region of the parameter space, these require the knowledge of other SUSY parameters. Especially in the extraction of the parameters as illustrated in Fig. 6, one should take the uncertainty on other SUSY parameters into account as a theoretical error, like the neglect of higher-order corrections to the Higgs mass. As for the ISR (initial-state

[9] For a comparison between the three-body and two-body $c\tilde{\chi}_1^0$ decays of $\tilde{t}_1$, as well as a general discussion of $\tilde{t}_1$ decays, see [20,33].

radiation), they should be easy to implement, and their effect should be similar to that in stop-pair production, considering that the reaction is an s-channel annihilation process; most importantly, this does not require the knowledge of any new SUSY parameter. In any case, the present analysis should at least give a rough indication of how to indirectly extract the heavy-stop mass and $\tan\beta$, provided these parameters yield a large enough cross section. Note also that, as Fig. 6 shows, for $\tan\beta > 3$, $m_{\tilde{t}_2}$ is given almost entirely by the $\tilde{t}_1\tilde{t}_1 h$ cross section and therefore one could, in a first approximation for such values of $\tan\beta$, make do without a precise knowledge of m_h. We should also mention that within the scenario we have pursued, $e^+e^- \to \tilde{t}_1\tilde{t}_1 Z$ can provide similar information [34] and thus can be used to strengthen further the conclusion of the present analysis. In most part of the present analysis we have not included LHC in the picture. It is clear that some of the parameters discussed here, and perhaps others, could also be measured at the LHC. For instance, a heavy stop with a mass up to one TeV can be produced and its mass measured. For the scenarios we have been entertaining in this paper, these heavier stops could trigger Higgs production through their decay into a lighter stop and a Higgs. For some of these configurations, the classic Higgs production through two-gluon with the subsequent decay of the Higgs into two-photon can be much suppressed [9]. Heavier stop production can then, among other processes, serve as an alternative to Higgs production [35].

Acknowledgements. We would like to thank the participants of the 2nd Joint ECFA/DESY Study on Physics a Linear Collider for their comments and interest. Abdel Djouadi also informed us of a calculation of $e^+e^- \to \tilde{t}_1\tilde{t}_1 h$ [36]. The work of V. L. is supported by a JSPS Fellowship (P97215). The work of T. K. is supported by the Ministry of Education, Science and Culture, Japan under Grant-in-Aid (N° 08640388).

References

1. J. Erler and P. Langacker, hep-ph/9809352.
2. See also H. Haber and R. Hempfling, Phys. Rev. Lett. **66** (1991) 1815. Y. Okada, M. Yamaguchi and T. Yanagida, Prog. Theor. Phys. **85** (1991) 1. R. Barbieri and M. Frigeni, Phys. Lett. **B258** (1991) 395.
3. J. Ellis, G. Ridolfi and F. Zwirner, Phys. Lett. **B262** (1991) 477.
4. M. Carena, J. R. Espinosa, M. Quirós and C. E. M. Wagner, Phys. Lett. **355B** (1995) 209. M. Carena, M. Quirós and C. E. M. Wagner, Nucl. Phys. **B461** (1996) 407.
5. M. Carena, P. H. Chankowski, S. Pokorski and C. E. M. Wagner, Phys. Lett. B **441** (1998) 205, hep-ph/9805349.
6. S. Heinemeyer, W. Hollik and G. Weiglein, Phys. Rev. **D58** (1998) 091701, hep-ph/9803277. The limiting case of vanishing stop mixing and large M_A and $\tan\beta$ has been considered by R. Hempfling and A. Hoang, Phys. Lett. **B331** (1994) 99.
7. For a review, see H. P. Nilles, Phys. Rep. **110** (1984) 1; R. Arnowitt, A. Chamseddine and P. Nath, *Applied N=1 Supergravity*, World Scientific, 1984.
8. See, for instance, J. R. Espinosa, Nucl. Phys. **B475** (1996) 273. J. M. Cline, M. Joyce and K. Kainulainen, Phys. Lett. **B417** (1998) 79, hep-ph/9708393. M. Carena, M. Quirós and C. E. M. Wagner, Nucl. Phys. **B524** (1998) 3, hep-ph/9710401. J. M. Moreno, M. Quirós and M. Seco, Nucl. Phys. **B526** (1998) 489, hep-ph/9801272. M. Laine and K. Rummukainen, Phys. Rev. Lett. **80** (1998) 5259, hep-ph/9804255. J. M. Cline, hep-ph/9810267.
9. A. Djouadi, Phys. Lett. **B435** (1998) 101, hep-ph/9806315.
10. A. Djouadi, J. Kalinowski and P. M. Zerwas, Mod. Phys. Lett. **A7** (1992) 1765 and Z. Phys. **C54** (1992) 255. S. Dittmaier, M. Krämer, Y. Liao, M. Spira and P. M. Zerwas, Phys. Lett. B **441** (1998) 383, hep-ph/9808433.
11. See, for instance, E. Accomando *et al.*, Phys. Rep. **299** (1998) 1, hep-ph/9705442.
12. R. Brinkman, G. Materlik, J. Rossbaach and A. Wagner, *Conceptual Design of a 500 GeV e^+e^- Linear Collider with Integrated X-ray Laser Facility*, DESY 1997–048/ECFA 1997–182. See also, the DESY/ECFA LC Workshop, http://www.desy.de/conferences/ecfa-desy-lc98.html.
13. Physics and technology of the Next Linear Collider: A Report submitted to Snowmass '96 by NLC ZDR Design Group and NLC Physics Working Group (S. Kuhlman *et al.*), hep-ex/9605011.
14. *Physics and Experiments with Linear Colliders*, 1. Finland: eds. R. Orava, P. Eerola and M. Nordberg, World Scientific, 1992. 2. Hawai: eds. F.A. Harris *et al.*,, World Scientific, 1994. 3. Japan: eds. A. Miyamoto and Y. Fujii, World Scientific, 1996.
15. For a study of stop-stop Higgs production at the LHC see, A. Djouadi, J. L. Kneur and G. Moultaka, Phys. Rev. Lett. **80** (1998) 1830, hep-ph/9711244.
16. J. L. Feng and M. J. Strassler, Phys. Rev. **D51** (1995) 4661, hep-ph/9408359; Phys. Rev. **D55** (1997) 1326, hep-ph/9606477. G. Moortgat-Pick, H. Fraas, A. Bartl and W. Majerotto, Eur. Phys. J. C **7** (1999) 113, hep-ph/9804306; Acta Phys. Pol. **B29** (1998) 1497, hep-ph/9803304. S.Y. Choi *et al.*, Eur. Phys. J. C **7** (1999) 123, hep-ph/9806279. V. Lafage *et al.*, hep-ph/9810504.
17. For the extraction of the SUSY parameters, see, T. Tsukamoto, K. Fujii, H. Murayama, M. Yamaguchi and Y. Okada, Phys. Rev. **D51** (1995) 3153. M. M. Nojiri, K. Fujii and T. Tsukamoto, Phys. Rev. **D54** (1996) 6756. For an extremely nice summary, see K. Fujii, in *Physics and Experiments with Linear Colliders*, Morioka, Japan, p. 283 *Op. cit.*
18. J. L. Feng, M. E. Peskin, H. Murayama and X. Tata, Phys. Rev. **D52** (1995) 1418.
19. M. M. Nojiri, Phys. Rev. **D51** (1995) 6281. M. M. Nojiri, K. Fujii and T. Tsukamoto, Phys. Rev. **D54** (1996) 6756.
20. For a compendium on the phenomenology of third-generation sfermions at linear colliders including decays, see W. Porod, Ph. D. Thesis, Wien Uni., 1998, hep-ph/9804208.
21. A. Bartl, et al., Z. Phys. **C76** (1997) 549, hep-ph/9701336.
22. A. Bartl, et al., hep-ph/9709252.
23. M. Drees and K. I. Hikasa, Phys. Lett. **B252** (1990) 127. W. Beenakker, R. Höpker and P. M. Zerwas, Phys. Lett. **B349** (1995) 463.
24. H. Eberl, A. Bartl and W. Majerotto, Nucl. Phys. **B472** (1996) 481. A. Arhib, M. Capdequi-Peyranère and

A. Djouadi, Phys. Rev. **D52** (1995) 1404. For a recent review on the SUSYQCD corrections to squark production and decays, see: A. Bartl *et al.*, hep-ph/9711464.
25. H. Haber, in *Perspectives in Higgs Physics II*, ed. G. L. Kane, World Scientific, Singapore, 1998.
26. W. Loinaz and J. D. Wells, Phys. Lett. B **445** (1998) 178, hep-ph/9808287.
27. M. Drees and K. Hagiwara, Phys. Rev. **D42** (1990) 1709. R. Barbieri, M. Frigeni, F. Giuliani and H. E. Haber, Nucl. Phys. **341** (1990) 309. M. Drees, K. Hagiwara and A. Yamada, Phys. Rev. **D45** (1992) 1725. D. Garcia and J. Solà, Mod. Phys. Lett. **A9** (1994) 211. P. H. Chankowski *et al.*, Nucl. Phys. **B417** (1994) 101. For earlier analyses see, R. Barbieri and L. Maiani, Nucl. Phys. **B224** (1983) 32. C. S. Lim, T. Inami and N. Sakai, Phys. Rev. **D29** (1984) 1488. Z. Hioki, Prog. Theor. Phys. **73** (1985) 1283. J. A. Grifols and J. Solà, Nucl. Phys. **B253** (1985) 47.
28. J. M. Frère, D. R. T Jones and S. Raby, Nucl. Phys. **B222** (1983) 11. M. Claudson, L. Hall and I. Hinchcliffe, Nucl. Phys. **B228** (1983) 501. C. Kounnas, A. B. Lahanas, D. V. Nanopoulos and M. Quirós, Nucl. Phys. **B236** (1984) 438. J. F. Gunion, H. E. Haber and M. Sher, Nucl. Phys. **B306** (1988) 1. P. Langacker and N. Polonsky, Phys. Rev. **D50** (1994) 2199. A. Strumia, Nucl. Phys. **B482** (1996) 24. For a recent summary, see J. A. Casas, hep-ph/9707475.
29. A. Kusenko, P. Langacker and G. Segre, Phys. Rev. **D54** (1996) 5824. A. Kusenko and P. Langacker, Phys. Lett. **B391** (1997) 29, hep-ph/9602414. A. Kusenko, nucl. Phys. Proc. Suppl. **52A** (1997) 67, hep-ph/9607287.
30. For a description of the program see, for example, M. Jimbo, H. Tanaka, T. Kaneko and T. Kon, Nucl. Phys. B **449** (1995) 49, hep-ph/9503363. J. Fujimoto *et al.*, Comput. Phys. Comm. **111** (1998) 185, hep-ph/9711283.
31. C. M. Holck (CDF Coll.), Abstract 652, ICHEP 98, Vancouver, BC, July 98.
32. K. Hikasa and M. Kobayashi, Phys. Rev. **D36** (1987) 724.
33. W. Porod and T. Wohrmann, Phys. Rev. **D55** (1997) 2907.
34. G. Bélanger, F. Boudjema, T. Kon and V. Lafage, in preparation.
35. G. Bélanger, F. Boudjema and K. Sridhar, in preparation.
36. A. Djouadi, private communication.